Macromolecules
ARTICLE

Macromolecules **2010**, *43*, 4223–4229 **4223**
DOI: 10.1021/ma100379j

Multi-Length Scale Morphology of Poly(ethylene oxide)-Based Sulfonate Ionomers with Alkali Cations at Room Temperature

Wenqin Wang,[†] Wenjuan Liu,[‡] Gregory J. Tudryn,[‡] Ralph H. Colby,[‡] and Karen I. Winey*[,†]

[†]*Department of Materials Science and Engineering, University of Pennsylvania, Philadelphia, Pennsylvania 19104-6272, and* [‡]*Department of Materials Science and Engineering and Materials Research Institute, The Pennsylvania State University, University Park, Pennsylvania 16802*

Received February 16, 2010; Revised Manuscript Received March 24, 2010

ABSTRACT: A series of Li-, Na-, and Cs-neutralized polyester ionomers with well-defined poly(ethylene oxide) (PEO) spacer lengths between sulfonated phthalates have been investigated by X-ray scattering at room temperature. As the spacer lengths are increased the PEO segments crystallize, as evidenced by multiple crystal reflections that are identical to those of pure poly(ethylene glycol) oligomers. This crystallization also produces multiple small-angle peaks, which correspond to the well-defined thickness of PEO crystallites. The ionomer peak ($q = 1-5$ nm^{-1}) is absent in the Na- and Cs-neutralized ionomers, while the Li-neutralized ionomers show peaks at $q = 2-3$ nm^{-1}, reminiscent of conventional ionic aggregates in ionomers. Detailed analysis of the normalized X-ray scattering intensity from these ionomers reveals a variety of ionic states that are highly dependent on the cation size. The states of ionic groups change from a majority of isolated ion pairs to aggregated structures as the cation size decreases from Cs to Li. These findings compare favorably with *ab initio* calculations.

Introduction

Ion-conducting polymers have been the subject of intensive research for potential applications in energy storage and conversion devices, such as rechargeable lithium ion batteries and fuel cells.[1−5] The conductivity of the material is determined by both the ion mobility and the total number of mobile charge carriers, which in turn depend on the primary chemical structures and the secondary structures, namely the morphologies. In order to understand the ion conduction mechanism, a comprehensive understanding of the multiscale structure is essential.

The most widely studied systems for lithium batteries are based on poly(ethylene oxide) (PEO), which can effectively solvate a variety of alkali and alkaline cations.[6−8] Most of the earlier work has been focused on mixtures of PEO with salts. FTIR and Raman studies have assigned various vibration bands of anionic groups, such as triflates and sulfonates, to free anion, cation−anion pairs, and aggregated structures.[9−11] In addition, the complexation of ether oxygens with cations results in conformational changes of the PEO polymer backbone, which yields indirect information about the cation environment.[11−13] X-ray diffraction studies have been focused mainly on crystalline PEO-salt complexes. Cations are found to be incorporated into the crystalline complex and form various crystalline structures with PEO chains.[14−16] It was recently demonstrated that polymer electrolytes of certain ordered crystalline structures can exhibit higher conductivity than disordered amorphous structures.[17] Although polymer/salt mixtures are able to provide reasonable conductivity, they suffer from undesirable concentration polarization, in which anions build up at the electrode/electrolyte interface due to their high mobility in the electrolyte and exclusion from the electrode.[18] The concentration polarization degrades battery performance.

*Corresponding author. Telephone: (215) 898-0593. Fax: (215) 573-2128. E-mail: winey@seas.upenn.edu.

Scheme 1. PEO-Based Sulfonated Polyester Ionomers with Well-Defined PEO Spacer (M_n = 400, 600, 1100, and 3300 g/mol, and m = 9, 13, 25, and 75)[a]

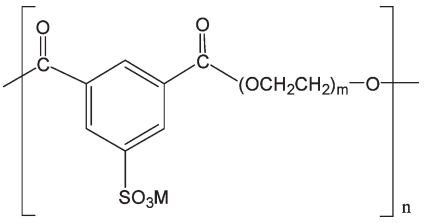

[a] M represents the cation (M = Li, Na, or Cs) associated with the sulfonate group.

Recently, there has been increasing interest in the study of single-ion conductors with anions fixed to the polymer backbone, because they can achieve a cation transference number of 1 and solve the concentration polarization problem.[18] However, most single-ion conductors show much lower conductivity than the polymer/salt mixtures. Dielectric spectroscopy studies on PEO-based sulfonated polyester and polyurethane ionomers indicate these materials have extremely low concentrations of conducting ions, and the conductivity exhibit a strong dependence on the glass transition temperature of ionomers.[19−21] A recent FTIR study on PEO-based sulfonated polyester ionomers neutralized by sodium cation showed no detectable free SO_3^- ions,[22] consistent with the dielectric studies. However, an overall picture of the morphology of these ionomers is still not available, and might hold the key to developing strategies to improve ion conductivity.

In this study, we analyze X-ray scattering data to determine the multiscale structure and ion association states of PEO-based sulfonated polyester ionomers with the structure shown in Scheme 1. A series of sulfonated polyester ionomers with well-defined PEO spacer lengths are investigated as a function of PEO segment length and alkali cation type. Here we focus on the room-temperature multiscale morphology of these ionomers.

Published on Web 04/14/2010

Table 1. Number Average Molecular Weight (M_n) Determined by ^{1}H NMR, and Glass Transition Temperature (T_g), Melting Temperature (T_m), and Percent Crystallinity Determined by DSC for PEO-based Ionomers and PEG Oligomers

notation	M_n, polymers (g/mol)	M_n, PEO spacer (g/mol)	T_g (°C) (DSC)	T_m (°C) (DSC)	% crystallinity
PEO400−100%Li	3300	400	12[b]	N/A	0
PEO400−100%Na	3400	400	22[b]	N/A	0
PEO400−100%Cs	4000	400	21[b]	N/A	0
PEO600−0%	6000	600	−46[b]	N/A	0
PEO600−100%Li	4500	600	−15[b]	N/A	0
PEO600−100%Na	4600	600	−6[b]	N/A	0
PEO600−100%Cs	5200	600	−3[b]	N/A	0
PEO1100−100%Li[a]	4500	1100	−36	32	8
PEO1100−100%Na[a]	4500	1100	−31	33	4
PEO1100−100%Cs[a]	4900	1100	−34	33	2
PEO3300−100%Na	18 800	3300	N/A	47	48
PEG2800	2800	N/A	N/A	58	91
PEG9900	9900	N/A	N/A	63	84

[a] In ref 23, these materials are labeled PE900−M (M = Li, Na or Cs), but more recent analysis has determined that the PEO spacer length is 1100 g/mol. [b] Values from ref 23.

Experimental Section

Materials. Poly(ethylene oxide) (PEO) based ionomers were prepared by a two-step catalyzed melt transesterification of poly(ethylene glycol) (PEG) oligomer diols of different molecular weights with dimethyl 5-sulfoisophthalate sodium salt to give ionomers of varying ion contents. The detailed synthesis procedures have been described in the previous publication.[23] ^{1}H nuclear magnetic resonance (NMR) is employed to verify the chemical structure and determine the number-average molecular weight (M_n) of the ionomers, Table 1. The molecular weights of PEO spacers are 400, 600, 1100, or 3300 g/mol, which were also determined by ^{1}H NMR. The cation was exchanged from sodium to lithium or cesium by aqueous diafiltration with an excess of LiCl or CsCl salts.[23] The concentrated ionomer solutions were then freeze-dried and vacuum-dried at 120 °C to constant mass. The ionomers are denoted as PEOx−yM, where x is the molecular weight of PEO spacers in g/mol, y is the percent of sulfonated phthalates over the total amount of phthalates in the ionomer, and M represents the cation (M = Li, Na or Cs). For example, PEO600−100%Na designates the ionomer with PEO spacer length of 600 g/mol and 100% sulfonated phthalates neutralized with Na. Note that all the ionomers studied in this paper are 100% sulfonated and fully neutralized with alkali metal cations; thus, y is always 100%.

In addition to these ionomers, we also investigated the X-ray scattering of PEO600−0% and poly(ethylene glycol) oligomers (PEG9900 and PEG2800). PEO600−0% is a neutral polymer that contains only noncharged phthalates between PEO spacers, and was synthesized by reacting PEG diols with dimethyl isophthalate.[23] PEG9900 (M_n = 9900 g/mol) and PEG2800 (M_n = 2800 g/mol) were supplied by Sigma-Aldrich and TCI America, Inc., respectively. The molecular weights of these PEG oligomers were determined by ^{1}H NMR.

Thermal Analysis. The glass transition temperatures (T_g) of the ionomers were determined by differential scanning calorimetry (DSC) during the second heating cycle from −90 to +200 °C. Both heating and cooling rates are 10 °C/min. The melting temperatures (T_m) and percent crystallinities for semicrystalline ionomers (PEO1100−100%M and PEO3300−100%Na) and PEG oligomers are determined from the first heating cycle at a heating rate of 10 °C/min for the purpose of maintaining similar thermal history as the samples used in X-ray scattering.

X-ray Scattering. Because of the hygroscopic nature and low T_g of these ionomers, the samples were handled very carefully to minimize the exposure of samples to moisture. The previously dried PEO-based ionomers were loaded into sandwich cells with mica windows, and further dried under vacuum at 70−80 °C for at least 2 days. The samples in the sandwich cell were gradually cooled down to room temperature under vacuum. The sandwich cell was then tightened and stored in a vacuum desiccator before being transferred to the X-ray vacuum chamber for data collection. It should be noted that PEO1100−100%M crystallizes very slowly at room temperature (~20 °C) compared to PEO3300−100%Na and PEG oligomers (PEG2800 and PEG9900) due to the presence of ions and the shorter PEO segment length. In order to study the crystalline structures of PEO1100−100%M, the dried materials were stored in a vacuum desiccator at room temperature for at least 1 week before data collection. As a comparison, PEG oligomers with M_n = 2800, and 9900 g/mol were also characterized by X-ray scattering. PEG oligomers were annealed in the vacuum oven at 70−80 °C for 24 h, and then slowly cooled down to room temperature under vacuum.

The multiangle X-ray scattering system (MAXS) used Cu Kα X-ray from a Nonius FR 591 rotating-anode generator operated at 40 kV and 85 mA. The bright, highly collimated beam was obtained via Osmic Max-Flux optics and triple pinhole collimation under vacuum. The scattering data were collected using a Bruker Hi-Star multiwire detector with sample to detector distances of 7, 11, 54, and 150 cm. The 2-D data reduction and analysis were performed using the Datasqueeze software.[24] Background scattering from an empty sandwich cell with mica windows are subtracted from the scattering data of samples. The normalized X-ray scattering data from PEO600−0% and PEO600−100%M were obtained by normalizing the scattering intensity by sample thickness, data collection time and percent of transmission.

***Ab Initio* Calculations.** All the calculations reported in this paper were carried out with the Gaussian03 program[25] with the anion on the polymer modeled by benzenesulfonate. Calculations for Li^+, Na^+, and K^+ used the B3LYP/6-31+G* basis set, which considers all electrons in its optimization of configurations. Cs^+ has many electrons, so the B3LYP/LANL2DZ basis set was used for all calculations involving Cs^+. Both methods use density functional theory with Becke's three-parameter hybrid method and the LYP correlation functional (B3LYP) as the exchange−correlation functional.[26−29] Configurations were optimized and calculations were made at 0 K in vacuum for ion pairs and quadrupoles. Limited calculations were also performed using the polarizable continuum model (PCM) developed by Tomasi,[30−33] which is a simple extension of the Onsager model[34] to nonspherical cavities, which contain the ions, ion pairs and quadrupoles. The PCM calculations indicate that the 0K/vacuum calculations underestimate the actual ion spacings of isolated ion contact pairs and quadrupoles by about 10% at 300 K. The spacings between electron-rich atoms in these structures are useful for our interpretation of X-ray scattering in the 13 $nm^{-1} < q <$ 20 nm^{-1} range for the amorphous ionomers.

Results and Discussion

Table 1 presents number-average molecular weight (M_n), glass transition temperature (T_g) and melting temperature (T_m) of ten

PEO-based ionomers, one neutral counterpart (PEO600−0% from condensing PEG600 oligomer with nonsulfonated phthalates), and two PEG oligomers studied in this paper. The T_g values of all the ionomers in Table 1 are below room temperature and increase with increasing ion content (decreasing PEO-spacer length). Since these ionomers have very low T_g and relatively low molecular weight, they are able to reach thermodynamic equilibrium rapidly. Previous rheological studies have shown that the terminal relaxation time of these materials is on the scale of 1 s or less at 30 °C.[23] The percent crystallinity is estimated by comparing the measured heat of melting (ΔH_m) with that of 100% crystalline PEO with molecular weight of 4000 g/mol (215.6 J/g).[35] The ionomers are amorphous when the PEO spacer length is 400 or 600 g/mol. As the PEO segment length increases to 1100 or 3300 g/mol, polymer chains partially crystallize. The percent crystallinity of PEO3300−100%Na is about 48%, and the percent crystallinities of PEO1100−100%M with different cations are all less than 10%. The presence of ionic groups in the polymer backbone greatly reduces the crystallinity and slows the crystallization kinetics of the PEO spacer. The PEO1100−100%M did not show any crystallization or melting transitions during the second heating cycle (10 °C/min) due to their slow crystallization rate.

The crystalline peaks from the four semicrystalline PEO-based ionomers are compared to the PEG oligomer with M_n = 9900 g/mol in Figure 1. All the scattering data presented in this paper are collected at room temperature. The crystalline reflections at 13.6, 16.5, and 18.5 nm^{-1} (labeled C, E, and F in Figure 1 and Table 2) correspond well to the main reflections of typical PEO crystals having a helical chain conformation and a monoclinic lattice.[36] Each unit cell consists of four helical molecules along the *c*-axis.[29] The helices adopt 7/2 conformations,[36] in which 7 monomer units are required to complete two revolutions along the helix. The monoclinic unit cell is defined by the following parameters: a = 0.805 nm, b = 1.304 nm, c = 1.948 nm, and β = 125.4°.[36,37] The

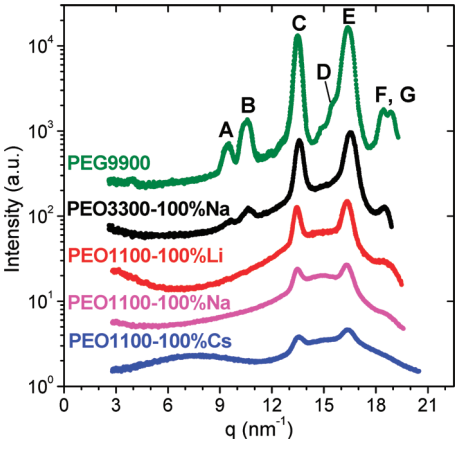

Figure 1. Comparison of crystal reflection peaks from semicrystalline PEO-based ionomers and the PEG9900 oligomer at room temperature. The X-ray scattering peaks labeled by letters correspond to crystalline PEO reflections; see details in Table 2.

crystallinity of ionomers decreases with decreasing PEO segment length and increasing cation size, as shown in the relative intensity of the crystal peaks. The *d*-spacings and corresponding crystalline reflections from both PEO-based ionomers and PEG oligomers are listed in Table 2. Some of the weaker crystal reflections are missing in the ionomer data due to their low crystallinity. The observed reflections in semicrystalline ionomers neutralized with three different cations (Li, Na, and Cs) and PEG oligomers are identical, indicating PEO spacers all crystallize into the monoclinic lattice structure of pure PEO. Because the lattice parameters remain unchanged in PEO-based ionomers, we conclude that the ions are excluded from the crystal and reside in the amorphous phase.

Figure 2 shows the room temperature X-ray scattering data from PEO*x*-100%M ionomers over a wide range of scattering angles. PEO400−100%M and PEO600−100%M are fully amorphous. These ionomers exhibit a strong peak at q ≈ 15 nm^{-1} corresponding to the amorphous halo of PEO. In semicrystalline ionomers (PEO1100−100%M and PEO3300−100%Na), the crystallinity is coupled with multiple small-angle peaks. Two different origins have been identified, as shown in Figure 2. The peak designated by "L" is assigned to the lamellar scattering, as observed in typical semicrystalline polymers and schematically drawn in Figure 3. The broad peak corresponding to the lamellar spacing in semicrystalline PEO3300−100%Na is obscured by the crystallite thickness peak (1) and the strong upturn at lower angles. The additional three peaks show a positional ratio of 1:2:3, as labeled in Figure 2, indicating a layered structure. The spacing of these layered structures (t_{expt}) is obtained from the periodic peak positions ($t_{expt} = \langle 2\pi/q_i \rangle$) and listed in Table 3. As a comparison, the lengths of 7/2 helices of the PEO spacers (t_{helix}) are calculated based on the monoclinic lattice parameters and reported in Table 3. On the basis of the consistency of t_{helix} with t_{expt} in Table 3, the higher order peaks (labeled 1, 2, 3 in Figure 2) are assigned to the scattering between the two amorphous−crystalline interfaces of each PEO crystallite and correspond to the crystallite thickness (t). This multiscale structure in semicrystalline ionomers is shown schematically in Figure 3. Note that the crystallite thickness increases with cation size (Li, Na, and Cs). It is expected that the ionic groups at the crystalline−amorphous interfaces also contributed to the scattering, thus the crystallite thickness obtained from X-ray scattering also includes the size of the ions. It is expected that the long PEO spacer might not be fully crystallized in PEO3300−100%Na, resulting in shorter periodicity in X-ray scattering ($t_{expt} < t_{helix}$). Connor et al. found by dynamic measurement that the crystallinity of PEG oligomers reached a maximum at M_n around 1000 g/mol.[38] This is because the number of lattice defects tends to increase with molecular weight while the packing problem of chain ends dominates in polymers of low molecular weight.

Typical semicrystalline polymers usually show only the L peak due to the polydispersity in crystallite thickness and limited contrast between the amorphous and crystalline domains. The appearance of multiple peaks in PEO-based ionomers is caused by well-defined crystallite thicknesses and the increased electron density difference provided by the cations. Typically, the

Table 2. Observed Crystalline Peaks in PEG Oligomers and PEO-Based Ionomers in Figure 1 and the Corresponding PEO Crystal Reflections[a]

peak	*d*-spacing[b] (nm)	reflections[36] (*hkl*)	PEG 2800, 9900	PEO1100−100%Li, Na, Cs	PEO3300−100%Na
A	0.59	020, $0\bar{2}0$	yes	no	yes
B	0.65	110, $\bar{1}10$, $\bar{1}\bar{1}0$, $1\bar{1}0$	yes	no	yes
C	0.46	120, $\bar{1}20$, $\bar{1}\bar{2}0$, $1\bar{2}0$	yes	yes	yes
D	0.40	004, $00\bar{4}$	yes	no	no
E	0.38−0.39	032, $0\bar{3}2$, 112, $1\bar{1}2$, $\bar{1}32$, $\bar{1}\bar{3}2$, $\bar{2}12$, $\bar{2}\bar{1}2$, $\bar{2}04$	yes	yes	yes
F, G	0.33−0.34	024, $0\bar{2}4$, $\bar{2}24$, $\bar{2}\bar{2}4$	yes	yes	yes

[a] "Yes" indicates that the peak is observed, and "no" indicates that the peak is not observed. [b] The *d*-spacing values are calculated by $2\pi/q$, where q is the position of peaks A−G.

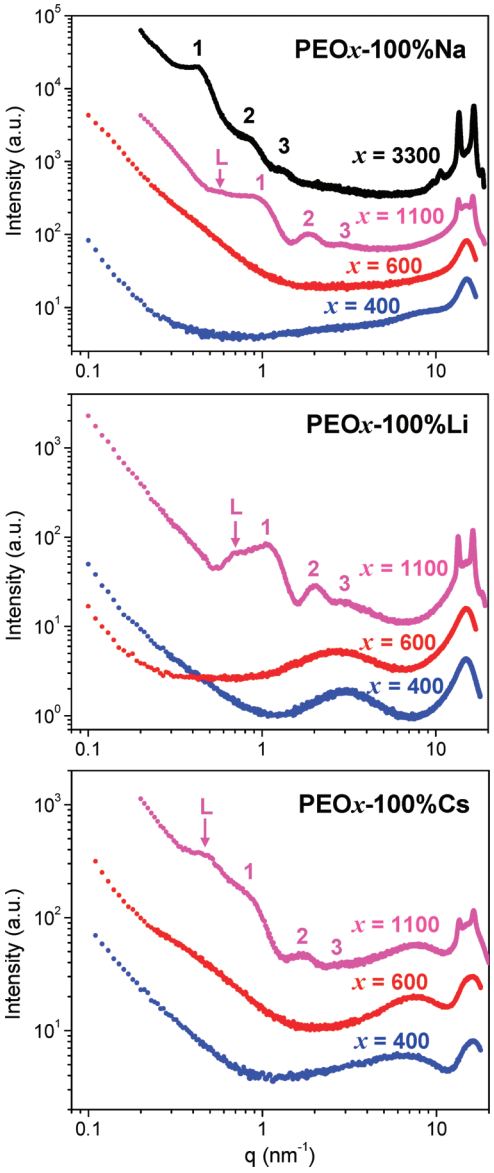

Figure 2. Multiangle X-ray scattering intensity as a function of scattering vector q on a log−log scale from PEOx−100%M ionomers with different PEO spacer lengths (x) and cations (M) at room temperature. The scattering peaks labeled L and numbers (1, 2, 3) correspond to the lamellar spacing (L) and the crystallite thickness (t_{expt}), respectively; see Table 3.

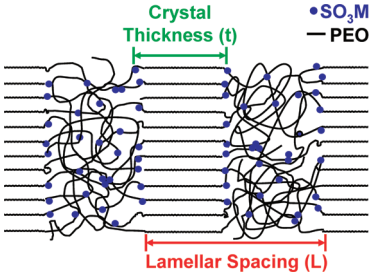

Figure 3. Schematic of the semicrystalline morphology of PEO-based ionomers showing crystalline lamellae-lamellae spacing (L) and well-defined crystallites of thickness (t).

thickness of polymer crystallites (t) is predominantly controlled by the crystallization temperature and time. In contrast, for PEO1100−100%M ionomers, the segment length is short enough that each segment of PEO chain between phthalates is *fully extended* in the crystallites. The experimental crystallite thickness t_{expt} is less than 12% different from the calculated value t_{helix}. Thus, the thickness of PEO crystallites in these ionomers is controlled by the well-defined PEO segment length.

On the other hand, the percent crystallinity of PEO1100-based ionomers is highly dependent on the thermal history and cation type. The lamellar spacing increases rather significantly with increasing cation size. The upper limit of the percent crystallinity in PEO1100−100%M ionomers can be estimated by t_{expt}/L_{expt}, which is 69%, 61%, 50% for ionomers neutralized with Li, Na, and Cs, respectively. Because of the presence of ionic groups, the actual percentages of crystallinity of these ionomers are all less than 10% and decrease with increasing cation size, Table 1. Moreover, the ionomers crystallize very slowly over several days at room temperature under vacuum. Increasing the cation size reduces both the crystallization rate and the percent crystallinity of the ionomer, because the larger cation generally requires more ether oxygen coordination in both amorphous state and PEO-salt crystalline complex.[39,40]

To further understand the multiscale crystalline structure in semicrystalline PEO-based ionomers, PEG oligomers with different molecular weights (2800 and 9900 g/mol) were also studied by X-ray scattering, see Figure 4. Both PEG oligomers show multiple peaks with positional ratios of 1:2:3 ... in this angular regime. These PEG oligomers show high percentages of crystallinity by DSC: 91% for PEG2800 and 84% for PEG9900. Thus, t_{expt} is comparable to L_{expt}, and, as a result, the lamellar-lamellar scattering peaks in the PEG oligomers are probably obscured by the crystallite thickness peaks due to their proximity in position. The size of the crystallites in PEG2800 obtained from X-ray scattering (t_{expt}) corresponds well with the calculated value based on the PEG2800 molecular weight (t_{helix}), Table 3. The oligomer chain of PEG2800 is fully extended when it crystallizes. In contrast, the longer oligomer PEG9900 forms folded structures, since $t_{helix} \approx 3t_{expt}$. The observed behavior (extended or folded

Table 3. PEO Crystallite Thickness (t) and Lamellar Spacing (L) from Calculation and X-ray Scattering Experiment

	m(PEO)[a]	t_{helix} (nm)	t_{expt} (nm)	L_{expt} (nm)	PEO chain
PEO1100−100%Li	25	7.0	6.2	9.0	extended
PEO1100−100%Na	25	7.0	6.8	11.2	extended
PEO1100−100%Cs	25	7.0	7.2	14.3	extended
PEO3300−100%Na	75	20.8	15.3		extended
PEG2800	64	17.8	19.3		extended
PEG9900	224	62.3	23.8		folded

[a] m denotes the degree of polymerization of the PEO spacer.

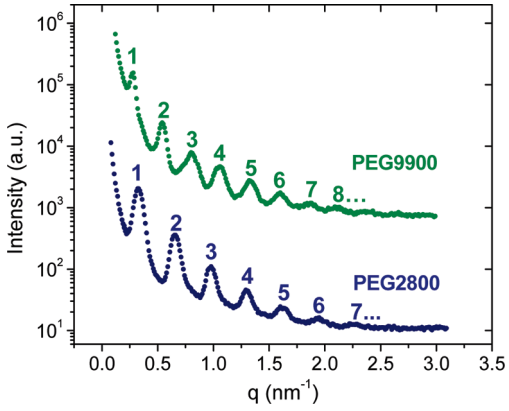

Figure 4. X-ray scattering intensity as a function of scattering vector q plotted in log−linear scale for PEG oligomers with different molecular weights at room temperature. The numbers correspond to higher order scattering from the crystallite thickness (t_{expt}), Table 3.

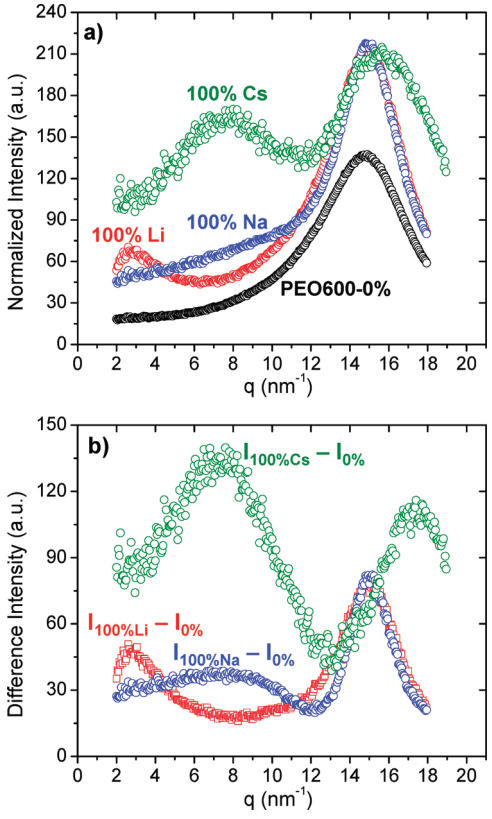

Figure 5. (a) Wide-angle X-ray scattering intensity at room temperature from PEO600−100%M (M = Li, Na, Cs) and PEO600−0% normalized by sample thickness, collection time, and percent of transmission. (b) Difference intensity of PEO600−100%M after subtracting scattering intensity of PEO600−0% from PEO600−100%M.

chain) in these two PEG oligomers is consistent with previous findings.[41,42] In particular, Sánchez-Soto et al. observed the melting temperature of PEO reached the plateau at the critical molecular weight of 4000 g/mol, which was interpreted as transition from extended chain to folded chain in PEO crystallites.[42]

The states of ions in PEO-based ionomers neutralized with different cations are quite different from conventional ionomers. Previous X-ray scattering data from a variety of model ionomers show an ionomer peak at $q = 1-5$ nm^{-1}.[43] Examples include Na- and Zn-neutralized poly(ethylene-*ran*-methacrylic acid) ionomers,[44,45] sulfonated polystyrene ionomers neutralized with Cu, Mg, Zn, Na, Ba, and Cs,[46,47] or Li-, Cs-, and Cu-neutralized poly(styrene-*ran*-methacrylic acid) ionomers.[48,49] PEO600−100%Li shows an ionomer peak at $q \approx 2.7$ nm^{-1} (Figure 2), indicating microphase separated structures with ~2.3 nm spacing. The peak shifts to higher q value (smaller interparticle spacing) as the PEO segment length decreases from 600 to 400 g/mol, meaning that the number density of ionic aggregates increases with ion content. PEO1100−100%Li also showed an ionomer peak, which overlaps with higher-order scattering peaks from crystal thickness and has been observed in thermally quenched PEO1100−100%Li when the ionomer was amorphous. The presence of a well-defined correlation scattering peak, as opposed to an asymmetric shoulder, upturn, or tail, suggests that the ionic aggregates are homogeneously distributed in the matrix and are of sufficiently high number density to generate interparticle scattering.

In contrast, the Na- and Cs-neutralized PEO-ionomers do not show any ionomer peak in Figure 2. The Cs-neutralized PEO-ionomers show a broad peak around 6−8 nm^{-1}. On the basis of the peak position and total ion concentration in these ionomers, the peak is attributed to the scattering from mostly isolated ion pairs. (Additional evidence will be presented later when we discuss Figure 5b.) Contrary to the Li-ionomers, the peak shifts to a lower q value (larger interparticle spacing) and broadens as the PEO segment is shortened, which is probably caused by the increasing fraction of Cs ions forming aggregates at higher ion content. As the ion pairs aggregated due to decreasing ethylene oxide (EO) /Cs ratio, the average correlation distance between scatters increased. Our results are consistent with previous spectroscopic study of PEO-based sulfonate ionomers, which found that the band due to aggregated sulfonate increased in intensity with increasing ion concentration.[22] Even though the PEOx−100%Na and PEOx−100%Cs ionomers do not exhibit an ionomer peak, these materials could still contain a small amount of randomly distributed ionic aggregates, as the subsequent analysis suggests.

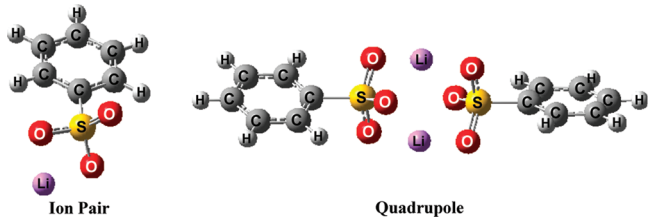

Figure 6. Simulation results for an ion pair and a quadrupole equilibrated at 0 K in vacuum using *ab initio* calculations.

To obtain quantitative comparison between the scattering data from ionomers neutralized with three different cations, the wide-angle X-ray scattering intensities of PEO600−100%M are normalized by sample thickness, data collection time and percent of transmission, as shown in Figure 5a. PEO600−100%M ionomers showed stronger amorphous peak intensity at 14−16 nm^{-1} compared to PEO600−0%, which is caused by the additional scattering from S, O, and metal cations. Figure 5b displays the difference scattering intensity of PEO600−100%M after subtracting the scattering from PEO600−0%, and shows apparent peaks at $q = 2-12$ nm^{-1} from PEO600−100%M. These peaks result from the interparticle scattering from closely assembled and strongly interacting ions in various associated states, such as isolated ion pairs, quadrupoles, or larger aggregates. Figure 6 shows equilibrated structures of an ion pair and a quadrupole generated by *ab initio* calculations of lithium benzenesulfonate.

The sharp peak centered at 2.7 nm^{-1} in PEO600−100%Li is virtually unchanged from Figure 5a to Figure 5b and indicated the presence of ionic aggregates, as discussed above. The broad peak centered at ~7 nm^{-1} from subtracted PEO600−100%Cs in Figure 5b corresponds to a correlation distance of 0.9 nm. If all the ionic groups form isolated ion pairs, the distance between ion pairs estimated from the total concentration of cations (~0.75 nm^{-3})[19] is ~1.1 nm by assuming simple cubic packing. Since the ion pairs are randomly distributed in the matrix rather than in a lattice, we expect the average distance between ion pairs to be slightly smaller than 1.1 nm. This estimate is comparable to the distance obtained from X-ray scattering, indicating the majority of the ions in PEO600−100%Cs exist in isolated ion pairs. However, due to the broadness of the difference peak, the presence of a small fraction of disordered ionic aggregates cannot be excluded.

The weak peak centered at 7 nm^{-1} from subtracted PEO600−100%Na is even broader than that from PEO600−100%Cs, suggesting a wider range of distributions of ionic states and correlation distances. The weakness of this peak corresponds to a smaller difference in electron density between SO_3Na and PEO. The asymmetry and broadness of the peak suggests that PEO600−100%Na contains both isolated ion pairs and some disordered ionic aggregates. Previous studies of PEO600−100%Na ionomers by FTIR have identified two different states

Table 4. *Ab Initio* Calculations of Interatomic Spacings at 0 K in Vacuum for Benzenesulfonate with Alkali Cations (M = Li^+, Na^+, K^+, or Cs^+)

			ion quadrupole		
cation	effective cation radius (nm)[a]	ion pair S−M (nm)	S−M (nm)	S−S (nm)	M−M (nm)
Li^+	0.076	0.24	0.29 (2), 0.25 (2)	0.41	0.35
Na^+	0.102	0.27	0.29 (4)	0.46	0.33
K^+	0.138	0.31	0.33 (4)	0.51	0.41
Cs^+	0.167	0.33	0.38 (4)	0.59	0.47

[a] Effective ionic radii are based on a six-coordination oxygen environment.[50]

of sulfonate groups, corresponding to a majority of isolated ion pairs (SO_3Na) and a considerable amount of aggregates (with higher frequency S−O stretching vibrations indicating $NaSO_3Na$).[22] Without subtracting the scattering from PEO600−0%, the peak for PEO600−100%Na is hidden underneath the broad amorphous peak due to its low intensity and proximity to the stronger amorphous peak. The intensity of this broad peak increases with ion content, as observed by comparing PEO600−100%Na and PEO400−100%Na at $q = 6-11$ nm^{-1} in Figure 2.

The peaks at 12−18 nm^{-1} in Figure 5b arise from interatomic scatterings of ionic groups in various states, because the contribution from amorphous PEO scattering has been subtracted. The peak at 15.0 nm^{-1} in PEO600−100%Li and Na corresponds to a correlation distance (d) of 0.42 nm, while PEO600−100%Cs shows $d = 0.36$ nm ($q = 17.4$ nm^{-1}). To facilitate interpretation, *ab initio* calculations at 0K in vacuum were made on ion pairs and quadrupoles of benzenesulfonate with various alkali cations (M), with the results shown in Table 4. In ion pairs, only the sulfur−cation (S−M) distances are shown, since sulfur has higher electron density than oxygen. In quadrupoles, three interatomic spacings are considered: sulfur-cation (S−M), sulfur−sulfur (S−S), and cation−cation (M−M). As expected, the S−M spacing of the isolated ion pairs are consistently smaller than the S−M spacings in quadrupoles, since the latter has cation−cation and sulfonate−sulfonate repulsions in addition to sulfonate−cation attractions. Ion pairs and quadrupoles of sulfonated dimethyl phthalate have also been calculated for comparison. Adding ester groups to the benzene ring changes electronic states of the benzene ring only slightly, because the charged sulfonate group dominates the electronic states. Thus, the relatively subtle effects of the ester groups cause little change to interatomic distances. For example, the Li sulfonated dimethyl phthalate pair has 0.5% larger Li−S spacing and the Li sulfonated dimethyl phthalate quadrupoles have 1.2% larger S−S spacing. These changes are well within uncertainties.

Interatomic distances at room temperature in the significantly more polar environment of our ionomers are expected to be ~10% larger than those in Table 4. To facilitate comparison with our X-ray scattering results at room temperature, we multiply the interatomic distances in Table 4 by 1.1 for the following discussion. The d value (0.42 nm) from X-ray scattering of PEO600−100%Li correlates best with the S−S spacing of the quadrupoles from *ab initio* calculations (0.41 nm × 1.1 = 0.45 nm), suggesting that S−S scattering in quadrupoles contributes the most to the peak at 15 nm^{-1} in PEO600−100Li. The higher q peak (with $d = 0.36$ nm) in PEO600−100%Cs is consistent with the S−Cs spacing (0.33 nm × 1.1 = 0.36 nm) in ion pairs. This is consistent with our interpretation above that ions in PEO600−100%Cs mainly form mostly ion pairs, while ions in PEO600−100%Li form aggregated structures, which by their nature could include quadrupoles. For PEO600−100% Na, the experimental d value (0.42 nm) lies between S−S spacing of the quadrupoles (0.46 nm × 1.1 = 0.51 nm) and M−M spacing of the quadrupoles (0.33 nm × 1.1 = 0.36 nm). Given that S and Na are close in electron density, the comparison with *ab initio* is inconclusive. More accurate prediction of the peak shape and intensity would require form factor and structure factor simulation, as well as the exploration of additional types of ionic assemblies.

Our results show that the size of the cation plays a critical role in the ionic states of PEO-based ionomers. This is different from conventional ionomers where the ionic aggregation behavior is relatively insensitive to the neutralizing cations.[45,47] The dependence of ionic association on the cation size in PEO-based ionomers is attributed to the interactions between the ether oxygens from PEO and the cations. The association energy of cations with anions and cations with ether oxygens increases with decreasing cation size to produce different coordination structures and local morphologies with different cation sizes. Our results from X-ray scattering are consistent with the previous findings by dielectric relaxation spectroscopy that showed the mobile ion concentration increased with increasing cation size in PEO-based ionomers.[21]

Conclusion

The multiscale morphologies of PEO-based sulfonated polyester ionomers have been investigated by X-ray scattering. The morphologies of ionomers are highly dependent on the PEO segment length and cation size. Increasing the PEO segment length results in the crystallization of PEO segments into monoclinic unit cells that are identical to PEG oligomers. Thus, the ionic groups (SO_3^- and M^+) are apparently excluded to the amorphous domains of these PEO-based ionomers, which is in contrast to traditional crystalline PEO/salt mixtures. The crystalline PEO segments form crystallites with well-defined thickness as exemplified by the higher order scattering peaks, where the crystallite thickness is defined by the PEO segment length. The presence of ionic groups reduces the percent of crystallinity and slows crystallization kinetics relative to PEO. Although PEO has been shown to have maximum crystallinity at M_n around 1000 g/mol,[38] our PEO1100−100%M ionomers crystallize over a period of several days at room temperature in dry conditions and only obtain crystallinity of ~10% or less.

These PEO-based ionomers exhibit a wider range of microphase segregation of ions from polymer backbones than is seen in conventional hydrocarbon-based ionomers,[43] because there is significant solvation interaction between the cations and ether oxygens. Our results showed the ionic states are highly dependent on the cation type, due to the different association energies of cations with anion and ether oxygens. PEO-based ionomers containing Li cations form ionic aggregates, while the majority of ionic groups in Cs-neutralized ionomers exist as isolated ion pairs. PEOx−100%Na ionomers have a broader range of local ionic states, including both isolated ion pairs as well as aggregated states. The conductivity of ionomers is highly dependent on the association states of the ions. These PEO-based ionomers do not have high conductivity due to the low concentrations of conducting free ions,[23] because most of the ions form bound states. To improve the ionic conductivity, bulky ions with weaker binding energy or/and more polar functional groups that can effectively solvate the ions need to be introduced into the polymer structure. Our results provide important insights regarding the

hierarchical structures of the ionomers for rational design of molecular structures to improve the ionic conductivity. Since the conductivity of ionomers is highly dependent on temperature, a thorough investigation of morphology as a function of temperature is underway and will be the subject of a future publication.

Acknowledgment. This work is supported by the Department of Energy, Office of Basic Energy Sciences, under Grant No. DE-FG02-07ER46409. The authors gratefully acknowledge Siwei Liang for assistance in NMR data collection and Shichen Dou for synthesis. We also thank Paul Heiney, Janna Maranas, Karl Mueller, James Runt, and Michelle Seitz for helpful discussions.

References and Notes

(1) Takeoka, S.; Ohno, H.; Tsuchida, E. *Polym. Adv. Technol.* **1993**, *4* (2−3), 53–73.
(2) Meyer, W. H. *Adv. Mater.* **1998**, *10*, 439–448 .
(3) Armand, M.; Tarascon, J. M. *Nature* **2008**, *451* (7179), 652–657.
(4) Hickner, M. A.; Ghassemi, H.; Kim, Y. S.; Einsla, B. R.; McGrath, J. E. *Chem. Rev.* **2004**, *104*, 4587–4611.
(5) Smitha, B.; Sridhar, S.; Khan, A. A. *J. Membr. Sci.* **2005**, *259* (1−2), 10–26.
(6) Wright, P. V. *Br. Polym. J.* **1975**, *7*, 319–327.
(7) Xu, K. *Chem. Rev.* **2004**, *104*, 4303–4417.
(8) Armand, M. B.; Chabagno, J. M.; Duclot, N. J., In *Fast Ion Transport in Solids*; Vashishta, P., Mundy, J. N., Shenoy, G. K., Eds.; North Holland: New York, 1979; p 131.
(9) Kakihana, M.; Schantz, S.; Torell, L. M.; Stevens, J. R. *Solid State Ionics* **1990**, *40−1*, 641–644.
(10) Huang, W. W.; Frech, R.; Wheeler, R. A. *J. Phys. Chem.* **1994**, *98*, 100–110.
(11) Rhodes, C. P.; Khan, M.; Frech, R. *J. Phys. Chem. B* **2002**, *106*, 10330–10337.
(12) Frech, R.; Huang, W. W. *Macromolecules* **1995**, *28*, 1246–1251.
(13) Frech, R.; Rhodes, C. P.; Khan, M. *Macromol. Symp.* **2002**, *186*, 41–49.
(14) Lightfoot, P.; Nowinski, J. L.; Bruce, P. G. *J. Am. Chem. Soc.* **1994**, *116*, 7469–7470.
(15) Lightfoot, P.; Mehta, M. A.; Bruce, P. G. *Science* **1993**, *262* (5135), 883–885.
(16) Andreev, Y. G.; Bruce, P. G. *Electrochim. Acta* **2000**, *45*, 1417–1423.
(17) Gadjourova, Z.; Andreev, Y. G.; Tunstall, D. P.; Bruce, P. G. *Nature* **2001**, *412* (6846), 520–523.
(18) Wright, P. V. *MRS Bull.* **2002**, *27*, 597–602.
(19) Fragiadakis, D.; Dou, S.; Colby, R. H.; Runt, J. *J. Chem. Phys.* **2009**, *130*, 064907.
(20) Fragiadakis, D.; Dou, S. C.; Colby, R. H.; Runt, J. *Macromolecules* **2008**, *41*, 5723–5728.
(21) Klein, R. J.; Zhang, S. H.; Dou, S.; Jones, B. H.; Colby, R. H.; Runt, J. *J. Chem. Phys.* **2006**, *124*, 144903.
(22) Lu, M.; Runt, J.; Painter, P. *Macromolecules* **2009**, *42*, 6581–6587.
(23) Dou, S. C.; Zhang, S. H.; Klein, R. J.; Runt, J.; Colby, R. H. *Chem. Mater.* **2006**, *18*, 4288–4295.
(24) Heiney, P. A. *Commission on Powder Diffraction Newsletter* **2005**, *32*, 9–11.
(25) Frisch, M. J.; et al.et al. *GAUSSIAN 03, Revision B.05*; Gaussian Inc.: Pittsburgh, PA, 2003.
(26) Becke, A. D. *J. Chem. Phys.* **1993**, *98*, 1372–1377.
(27) Becke, A. D. *Phys. Rev. A* **1988**, *38*, 3098–3100.
(28) Lee, C. T.; Yang, W. T.; Parr, R. G. *Phys. Rev. B* **1988**, *37*, 785–789.
(29) Stephens, P. J.; Devlin, F. J.; Chabalowski, C. F.; Frisch, M. J. *J. Phys. Chem.* **1994**, *98*, 11623–11627.
(30) Mennucci, B.; Tomasi, J. *J. Chem. Phys.* **1997**, *106*, 5151–5158.
(31) Cances, E.; Mennucci, B.; Tomasi, J. *J. Chem. Phys.* **1997**, *107*, 3032–3041.
(32) Cossi, M.; Barone, V.; Mennucci, B.; Tomasi, J. *Chem. Phys. Lett.* **1998**, *286*, 253–260.
(33) Cossi, M.; Scalmani, G.; Rega, N.; Barone, V. *J. Chem. Phys.* **2002**, *117*, 43–54.
(34) Onsager, L. *J. Am. Chem. Soc.* **1936**, *58*, 1486.
(35) Beaumont, R. H.; Clegg, B.; Gee, G.; Herbert, J. B. M.; Marks, D. J.; Roberts, R. C.; Sims, D. *Polymer* **1966**, *7*, 401–417.
(36) Zhu, L.; Cheng, S. Z. D.; Calhoun, B. H.; Ge, Q.; Quirk, R. P.; Thomas, E. L.; Hsiao, B. S.; Yeh, F. J.; Lotz, B. *J. Am. Chem. Soc.* **2000**, *122*, 5957–5967.
(37) Takahash., Y.; Tadokoro, H. *Macromolecules* **1973**, *6*, 672–675.
(38) Connor, T. M.; Williams, G.; Read, B. E. *J. Appl. Chem. USSR* **1964**, *14* (2), 74.
(39) Besner, S.; Prudhomme, J. *Macromolecules* **1989**, *22*, 3029–3037.
(40) Thomson, J. B.; Lightfoot, P.; Bruce, P. G. *Solid State Ionics* **1996**, *85*, 203–208.
(41) Godovsky, Y. K.; Garbar, N. M.; Slonimsk, G. *J. Polym. Sci., Part C: Polym. Symp.* **1972**, *38*, 1–12.
(42) Sanchez-Soto, P. J.; Gines, J. M.; Arias, M. J.; Novak, C.; Ruiz-Conde, A. *J. Therm. Anal. Calorim.* **2002**, *67*, 189–197.
(43) Eisenberg, A.; Kim, J.-S. *Introduction to Ionomers*; John Wiley & Sons: New York, 1998.
(44) Marx, C. L.; Caulfield, D. F.; Cooper, S. L. *Macromolecules* **1973**, *6*, 344–353.
(45) Yarusso, D. J.; Cooper, S. L. *Polymer* **1985**, *26*, 371–378.
(46) Yarusso, D. J.; Cooper, S. L. *Macromolecules* **1983**, *16*, 1871–1880.
(47) Zhou, N. C.; Chan, C. D.; Winey, K. I. *Macromolecules* **2008**, *41*, 6134–6140.
(48) Eisenber., A.; Navratil, M. *Macromolecules* **1974**, *7*, 90–94.
(49) Wang, W.; Chan, T. T.; Perkowski, A. J.; Schlick, S.; Winey, K. I. *Polymer* **2009**, *50*, 1281–1287.
(50) Shannon, R. D. *Acta Crystallogr., Sect. A* **1976**, *32*, 751–767.